DOT/FAA/AR-04/2

Office of Aviation Research
Washington, D.C. 20591

Bulging Factor Solutions for Cracks in Longitudinal Lap Joints of Pressurized Aircraft Fuselages

June 2004

Final Report

This document is available to the U.S. public
Through the National Technical Information Service
(NTIS), Springfield, VA 22161.

U.S. Department of Transportation
Federal Aviation Administration

NOTICE

This report is available at the Federal Aviation Administration William J. Hughes Technical Center's Full-Text Technical Reports page: actlibrary.tc.faa.gov in Adobe Acrobat portable document format (PDF).

Technical Report Documentation Page

1. Report No.	2. Government Accession No.	3. Recipient's Catalog No.
DOT/FAA/AR-04/2		

4. Title and Subtitle	5. Report Date
BULGING FACTOR SOLUTIONS FOR CRACKS IN LONGITUDINAL LAP JOINTS OF PRESSURIZED AIRCRAFT FUSELAGES	June 2004
	6. Performing Organization Code

7. Author(s)	8. Performing Organization Report No.
Anisur Rahman*, John Bakuckas, Jr., and Catherine Bigelow	

9. Performing Organization Name and Address	10. Work Unit No. (TRAIS)
*NAVAIR Tactical Aircraft Code 43310 Building 378-2 NAS North Island San Diego, CA 92135 **Federal Aviation Administration William J. Hughes Technical Center Airport and Aircraft Safety Research and Development Division Airworthiness Assurance Branch Atlantic City International Airport New Jersey 08405	11. Contract or Grant No.

12. Sponsoring Agency Name and Address	13. Type of Report and Period Covered
U.S. Department of Transportation Federal Aviation Administration Office of Aviation Research Washington, DC 20591	Final Report
	14. Sponsoring Agency Code ANM-100

15. Supplementary Notes

The FAA William J. Hughes Technical Center COTR was John Bakuckas.

16. Abstract

This report is a compilation of bulging factor solutions obtained at the Federal Aviation Administration William J. Hughes Technical Center for cracks in typical transport category aircraft. The solutions were obtained for longitudinal cracks in the critical rivet row of longitudinal lap splice joints. Both unstiffened and frame- and longeron-stiffened configurations were considered. The loading, crack length, skin thickness, substructure spacing, and properties were varied. Baseline solutions for cracks in an unstiffened shell were also obtained. The results from these studies are compiled in this report, and the effects of the parameters that were varied on the bulging factor are discussed.

17. Key Words	18. Distribution Statement
Bulging factor solutions, Stress intensity factors, Pressurized aircraft fuselage, Longitudinal lap splice joint	This document is available to the public through the National Technical Information Service (NTIS) Springfield, Virginia 22161

19. Security Classif. (of this report)	20. Security Classif. (of this page)	21. No. of Pages	22. Price
Unclassified	Unclassified	37	

ACKNOWLEDGEMENTS

This research was partially supported by the National Computational Science Alliance and used the Silicon Graphics Origin 2000 Distributed Shared Memory System at the University of Illinois, Urbana-Champaign. Anisur Rahman would like to express sincere appreciation to the Federal Aviation Administration William J. Hughes Technical Center for support of this work through Grant (00-G-030) to Drexel University. The Naval Air Systems Command (NAVAIR), U.S. Department of Defense, where Anisur Rahman is currently employed, has funded the time to summarize this work, and this support is also gratefully acknowledged.

TABLE OF CONTENTS

LIST OF FIGURES

LIST OF TABLES

EXECUTIVE SUMMARY

Longitudinal cracks in pressurized aircraft fuselage structure are subjected complex stress and displacement fields resulting in nonlinear out-of-plane deformations. This so-called bulging effect can significantly elevate the stress-intensity factor (SIF) at the crack tip and reduce the residual strength. One measure of the bulging effect is the bulging factor, which is the ratio of the SIF at the tip of a longitudinal crack in the fuselage to the SIF for the same crack in a flat panel. The damage tolerance design philosophy requires realistic stress state determination in the vicinity of cracks in airframe fuselages.

This report is a compilation of bulging factor solutions obtained at the Federal Aviation Administration William J. Hughes Technical Center for cracks in typical transport category aircraft. The solutions were obtained for longitudinal cracks in the critical rivet row of longitudinal lap splice joints. Both unstiffened and frame- and longeron-stiffened configurations were considered. The loading, crack length, skin thickness, substructure spacing, and properties were varied. Baseline solutions for cracks in an unstiffened shell were also obtained. The results from these studies are compiled in this report, and the effects of the parameters that were varied on the bulging factor are discussed.

INTRODUCTION

The evolution of cracks in a pressurized fuselage structure is a complex process due to the biaxial and internal pressure loads and the structural configuration. The response of such cracks is characterized by large out-of-plane deformations or bulging of the surfaces of the crack, as illustrated in figure 1, which develop local membrane and bending stresses. The definition for bulging factor used in this study derives from the definition that is used for unstiffened shells. For unstiffened shells, the bulging phenomena is often quantified in terms of a bulging factor defined as the ratio of the stress-intensity factor (SIF) of a curved shell to the stress-intensity factor of a flat panel:

$$\beta = \frac{K_{curved}}{K_{flat}} \tag{1}$$

Thus, for unstiffened shells the bulging factor, β, can be applied to the SIF of a flat plate to obtain the SIF for a curved shell with the same crack. The definition adopted in this study is identical to that shown in equation 1, with the exception that in K_{curved}, the effect of stiffeners is also taken into account. To accurately determine the effect of crack bulging on crack growth in fuselage structures, calculations of the bulging factors for the fuselage configurations used in industry are needed. The bulging factor for fuselage structures is a nonlinear function of the applied pressure, material properties, and geometric parameters, including the fuselage radius, fuselage thickness, and crack length. To accurately model bulging of cracks, including the out-of-plane deformation, large displacement theory and geometric nonlinearities must be considered.

Several studies have been conducted to characterize bulging cracks [1-6]. However, most work done to date has been for unstiffened shells. Early works of Folias [1] provided the first analytical expressions for bulging factors based on linear elastic theory. Numerical analysis by Erdogen and Kibler [2], using linear elastic fracture mechanics, support the expressions developed by Folias. However, later work conducted by Riks [3] and Ansell [4], using geometric nonlinear finite element analysis, demonstrated that the bulging phenomena was a nonlinear problem and that large deformations need to be considered in order to appropriately characterize bulging cracks. It was shown that the SIF for a given crack configuration increased with applied pressure and the value was smaller than the value using linear elastic theory. The work of Chen and Schijve [5] considered the problem from a fracture mechanics, energy balance approach accounting for the nonlinear deformation in the vicinity of the crack using a semiempirical formulation. By correlating with experiments, Chen and Schijve [5] developed an expression for the bulging factor, which was in good agreement with the results published by Riks [3] and Ansell [4].

Due to the complexities of analyzing bulging cracks, a wide range of SIF for bulging cracks are not available. Without SIF, accurate damage tolerance assessments for a broad spectrum of crack configurations in aircraft fuselage structures are difficult. Only a handful of studies have been done for stiffened shells [3-5]. One of these was carried out by the Federal Aviation Administration, in which Bakuckas et al. [6] investigated the effect of bulging on curved panels that were both unstiffened and stiffened with straps. The present study builds upon this work

and looks into the effect of bulging on a cracked longitudinal lap splice joint. An area of particular concern is the critical rivet row in the longitudinal lap splice joint, which is 1 of the 16 critical areas identified by the Airworthiness Assurance Working Group that is susceptible to widespread fatigue damage [7]. No published solutions for bulging factors for cracks in a longitudinal lap splice joint exist. In the current study, a typical fuselage with a longitudinal lap splice joint with a crack in its critical rivet row was selected, as shown in figure 1. The effects of the presence of the lap splice, the stringers, and the frames on the bulging factor were examined. The current results will help in evaluating the need to incorporate bulging factors in the damage tolerance studies and residual strength analysis codes of aircraft fuselage design and repair.

COMPUTATIONAL METHODOLOGY

COMPUTING THE BULGING FACTOR.

In this study, the Modified Crack Closure Integral (MCCI) method was used to calculate the SIF. In the MCCI method, it is assumed that the energy released during crack extension is the same as the work that would be needed to close the crack, and that the energy released can be partitioned into four components of SIF [8-10]. The four SIF components consist of two in-plane SIFs, K_1, and K_2, due to the opening or tension mode and the shearing mode, respectively. The other two SIFs, k_1, and k_2, called the Kirchoff SIFs, are due to the symmetric bending and unsymmetric bending loads, respectively. The loading modes are shown in figure 2. The MCCI method approximates the work needed to close the crack using the local crack tip displacements and forces. The displacements and forces at the nodes of the four elements surrounding the crack tip were obtained from the finite element results for each crack length, as shown in figure 3. The work, W_i, done to close a crack of length, Δa, for the ith degree of freedom is given by [8]:

$$W_i = \frac{1}{2t\Delta a}\left[F_i^{close}\left(u_i^{top} - u_i^{bot}\right)\right], \; i = 1, \ldots, 6 \tag{2}$$

where, t is the thickness of the panel, F is the force needed to close the crack surfaces, u is the displacement component on each node on the surface of the crack, and i denotes the degree of freedom. The total amount of work necessary to close a crack by Δa is numerically equal to the total amount of strain energy released when the crack grows by Δa. The strain energy release rate is related to the SIF using the following mapping:

$$W_2 + W_6 = \frac{K_1^2}{E} \tag{3}$$

$$W_1 = \frac{K_2^2}{E} \tag{4}$$

$$W_4 = \frac{k_1^2 \pi}{3E}\left(\frac{1+\nu}{3+\nu}\right) \tag{5}$$

and,

$$W_3 + W_5 = \frac{k_2^2}{3E}\left(\frac{1+\nu}{3+\nu}\right) \tag{6}$$

here, E is the modulus of elasticity, and ν is Poisson's ratio.

In the configurations presented in this report, the mode 1 SIF, K_1 was the dominant of the four SIFs, and this was the component that was used to determine the bulging factor. Thus, in this report, the bulging factor is expressed by:

$$\beta = \frac{K_{1\ curved}}{K_{1\ flat}} \tag{7}$$

where, $K_{1\ curved}$ is the mode 1 SIF for a crack in the curved fuselage panel, and $K_{1\ flat}$ is the mode 1 SIF for the same crack configuration in an infinite panel under a remote tensile stress equal to the hoop stress in the curved panel:

$$K_{1\ flat} = \frac{pR}{t}\sqrt{\pi a} \tag{8}$$

Here, a is the half crack length, p is the internal pressure, R is the fuselage radius, and t is the skin thickness.

VERIFICATION STUDIES.

To verify the computational approach and to ensure sufficient fidelity in the finite element mesh, a problem with a known solution was modeled first: a pressurized unstiffened cylinder with a radius R of 64.96 in. (1650 mm). A longitudinal crack of length $2a$ = 7.874 in. (200 mm) was modeled. The solution of this problem can be obtained from the work of Bakuckas and Chen [5, 6, 11]. Bakuckas solved the problem using geometrically global-local hierarchical finite element approach and used the J-integral to calculate the SIF. Chen combined the analytical results of Ansell [4] and Riks [3] with test results and presented the bulging factors in the form of a semiempirical equation given by:

$$\beta = \sqrt{1 + \frac{5}{3\pi}\cdot\frac{Eta}{R^2 p}\cdot\frac{0.316}{\sqrt{1+18\chi}}\tanh\left(0.06\cdot\frac{R}{t}\cdot\sqrt{\frac{pa}{Et}}\right)} \tag{9}$$

Here, E is the tensile modulus of the cylindrical shell, t is the thickness, R is the radius of curvature, p is the internal pressure, and a is the half crack length. χ is a biaxiality ratio and is given by:

$$\chi = \frac{\sigma_{long}}{\sigma_{hoop}} \tag{10}$$

In the verification studies, the finite element analysis was performed by using ABAQUS [12]. The MCCI method was used to obtain the mode 1 SIF (K_1) and equation 9 was used to obtain the bulging factor. Figure 4 shows the plot of the bulging factor as a function of pressure. These solutions are within 1% of the values reported by Bakuckas et al. [6] and 3% of values obtained from Chen and Schijve's [5] semiempirical equation given by equation 9.

GEOMETRY AND CONFIGURATION.

Once the procedure was verified, the methodology was used to analyze bulging effects in a fuselage structure typical of a transport category aircraft. In this study, for all analyses, a representative fuselage radius of 80 in. was used. Four fuselage configurations, as shown in figure 5, were studied. The first was an unstiffened fuselage with a longitudinal crack, but with no lap splice joint or stiffeners. The second configuration was an unstiffened fuselage with a longitudinal lap splice joint, but without any stiffening. The two skins on different sides of the lap joint were attached by three rows of rivets. The rivet pitch was 1 in. with a half-inch edge distance. The rivets were modeled with a circular cross-section and a diameter of 0.0974 in. A crack was placed in the critical outer rivet row of the lap splice joint. In the third configuration, the fuselage with the longitudinal lap splice joint was stiffened with stringers (longitudinal-stiffening element) and the final configuration, the fuselage was fully stiffened with both stringers and frames (hoop-stiffening element). For this fully stiffened configuration, the crack was placed at mid-bay. The four fuselage configurations are shown in figure 5. The skin was made of 2024 aluminum alloy with a thickness of 0.048 in.

The stiffener configurations were selected to represent a typical transport category aircraft. The stringers were spaced at 10-in. intervals, and the frames were spaced 20 in. apart. The stringers have a hat configuration and the frames have a Z-configuration. The schematic of the cross-sections are shown in figure 6. The stiffeners were characterized using a stiffening ratio that relates the cross-section area of the stiffener to the skin thickness and stiffener spacing. This quantity has been identified as having the most influence on SIF and, hence, the bulging factor in the global sense [4]. The stiffening ratio is given by:

$$\gamma = \frac{A_s}{A_s + Lt} \tag{11}$$

where, A_s is the stiffener cross-sectional area, L is the stiffener spacing, and t is the skin thickness. A stiffening ratio of 0.2 was used for frames and 0.26 was used for stringers.

Six different crack lengths were studied in this work. The half-crack lengths of the crack studied are 1, 2, 6, 8, 10, and 12 in. A total of 18 different cases were analyzed[1]. The rivets at locations on the crack were assumed to be completely broken. In the fully stiffened configuration, the crack was in the mid-bay.

[1] Not all crack lengths were studied for every configuration.

FINITE ELEMENT ANALYSIS.

A geometrically nonlinear finite element analysis was conducted using the commercial finite element package ABAQUS [12]. Taking advantage of symmetry, only one-quarter of the unstiffened fuselage panel, as shown in figure 5(a), and one-half of the panels with longitudinal lap splice joints, as shown in figures 5(b) through 5(d), were modeled. The fuselage skin was modeled using four-noded shell elements with reduced integration. The stiffeners (stringers and frames) were modeled using beam elements having the cross-sectional properties discussed above and shown in figure 6. Beam elements were used to model the rivets that connected the substructures with the skin and the substructures to one another. To simplify the modeling, the rivet holes were not modeled. The semi-empirical equation developed by Swift [13] was used to calculate the shear stiffness of the beams, where the rivet shear stiffness is given by:

$$k_{shear} = \frac{E' d}{5 + 0.8\left(\frac{d}{t} + \frac{d}{t_s}\right)} \tag{12}$$

Here, $E' = 10.5\times10^6$ psi is the skin modulus, $d = 0.1875$ in. is the rivet diameter, $t = 0.048$ in. is the thickness of the first skin, and $t_s = 0.048$ in. is the thickness of the second skin. Table 1 lists the mechanical properties [14] used for skin, doublers, frames, and stringers. The crack configurations were simulated using pairs of coincident nodes along the shared edges of two rows of elements, as shown in the detailed view in figure 7. An orthogonal mesh was used in the immediate vicinity of the crack tips where the size of the elements were at least 0.25 in.

The boundary conditions applied are shown schematically in figure 7. Symmetry conditions were applied on the two longitudinal edges and one hoop edge perpendicular to the crack face and center of the crack. In the remaining side only the rotations about the z- and θ axes were constrained. Load was applied incrementally, loading the model to 10 psi and the bulging factor was calculated at each increment. The mode I SIF obtained from the finite element analysis was used as $K_{1\ curved}$ in equation 7 to calculate the bulging factor. The SIF for a flat plate was obtained from reference 14 and is given by:

$$K_{1\ flat} = \frac{pR}{t}\sqrt{\pi a} \tag{13}$$

Here, p is the internal pressure, R is the fuselage radius, and t is the skin thickness. The crack was grown by generating additional nodes in front of the crack tip and splitting the elements. As the crack progressed through the rivets, the rivets were assumed to be completely broken and unable to carry any load.

RESULTS AND DISCUSSIONS

The results are presented in terms of the bulging factor, β, as a function of the applied internal pressure. The first set of analyses is for the baseline configuration, an unstiffened fuselage with a central crack. The bulging factor for this configuration is plotted as a function of internal

pressure, as shown in figure 8. Results showed, that for all crack lengths, the bulging factor decreases as the internal fuselage pressure increases. This nonlinearity has been attributed to the straightening or tightening of the crack faces in the hoop direction as the pressure increases, which was also reported by other authors [3-6]. The variation of the bulging factor increases as the crack length increases. For the smallest crack length analyzed (a = 1 in., where a is the half-crack length), the bulging factor is practically constant at 1.2; whereas, for the longest crack length analyzed (a = 8 in.), the bulging factor varies between 2.5 and 4.0 for the pressure considered. Thus, the bulging phenomenon in unstiffened cylindrical shells becomes more geometrically nonlinear as the crack grows. The results for all the bulging factors calculated for longitudinal cracks in unstiffened fuselages, as shown in figure 8, are presented in tabular form in tables 2 through 6. Each table presents the bulging factor as a function of pressure for a given crack length. In addition to the bulging factor, the tables also list the four Kirchoff SIFs. One may observe that all the values of K_2 and k_2 are identically zero. This is to be expected because the baseline configuration is symmetric about the crack plane. K_2, and k_2 are the SIF corresponding to antisymmetric membrane and antisymmetric bending and symmetry dictates that these values are identically zero.

Figure 9 depicts the bulging factors as a function of pressure for an unstiffened fuselage configuration with a longitudinal lap splice joint. The crack was placed in the outermost critical rivet row. Five different cracks with half-lengths of a = 1, 2, 4, 6, and 8 in. were considered. The trends in the bulging factor plots are similar to the baseline case presented in figure 8, but the magnitudes are slightly lower. The presence of the riveted lap splice shields the crack and provides some stiffening effect. Compared to the baseline case, at an applied pressure of 10 psi, the bulging factor decreased 16% and 5% for a crack length of a = 1 and 8 in., respectively. Thus, the stiffening effect of the lap splice is less significant at longer crack lengths and at higher applied pressures. The bulging factors and the Kirchoff SIFs for the configurations and crack lengths, presented in figure 9 are tabulated in tables 7 through 11. From the tabulated values of the Kirchoff SIFs, one may observe that because of the eccentricity of the lap splice joint and the load transfer through rivets, the symmetry about the crack plane is lost. Figure 10 depicts all the Kirchoff SIFs for a crack with a half-length of 8 in. for this configuration. It can be observed that due to lack of symmetry about the crack plane, the values of K_2, and k_2 are nonzero. However, the SIF is still mode 1 (K_1) dominant.

The next set of results is for the longitudinally stiffened lap joint, as shown in figure 11. For this case, the stringer spacing is 10 in. The presence of stringers provides additional stiffness to the configuration. In the configuration analyzed, the lap splice stringer runs parallel to the crack at a distance of one rivet pitch. This stringer locally resists the out-of-plane deformation of the crack faces, resulting in a decrease in bulging factor compared to unstiffened baseline and lap splice cases. This local effect increases as the crack length increases. A nearly constant decrease in the bulging factor was obtained for all crack lengths analyzed. Compared to the baseline case, the bulging factor was reduced by 26% and 29% for a crack length of a = 1 and 8 in., respectively. The Kirchoff SIFs for all the configurations shown in figure 11 are given in tables 12 through 16.

In the final set of analyses, the fuselage was stiffened in both the longitudinal and hoop directions. The bulging factors for this configuration are presented as a function of pressure in figure 12. Here, seven different crack lengths were considered, a = 1, 2, 4, 6, 8, 10, and 12 in., and the frame spacing was 20 in. Thus, the smallest crack analyzed, a = 1 in., is quite remote

from the frames. A crack of a = 10 in. is equal to the width of the bay, and a = 12 in. represents a crack that is wider than the bay. For crack lengths longer than the frame spacing, the frame remained intact. The addition of the frames added stiffness to the fuselage and reduced the bulging factor compared to the results obtained for the previous longitudinally stiffened case.

The effect of the frames increased for longer crack lengths. For the smallest crack analyzed, a = 1 in., where the crack was quite remote from the frame, the bulging factor was reduced by 7% at p = 10 psi compared to the longitudinally stiffened case. The longer the crack, i.e., the crack tip is closer to the frame, the greater the reduction in the bulging factor. For a = 8 in., the reduction is almost 13% compared to the longitudinally stiffened case. At a given pressure, the bulging factor increased with crack length until it reached a maximum value when the crack length was equal to the frame spacing. For cracks longer than the frame spacing, the bulging factor decreased due to the stiffening effect of the intact frame. This behavior is further illustrated in figure 13, where the bulging factor is plotted as a function of half-crack length for different internal fuselage pressure. Similar phenomenon was observed by Bakuckas, et al. [6] for bulging cracks in stiffened shells with hoop tear straps. The bulging factors and the Kirchoff SIFs for the configurations and crack lengths presented in figure 12 are tabulated in tables 17 through 23.

The effect of configuration on the bulging factor is summarized in figures 14 and 15 for crack length a = 1 and 8 in., respectively. For the configurations analyzed, bulging factors were the highest for the baseline case and then reduced with each additional stiffening element. In all cases, the lap joint provided some stiffening effect, reducing the bulging factor compared to the baseline case. In addition, the results from longer cracks exhibit more geometric nonlinearity than results from shorter cracks. As shown in figure 14 for shorter crack lengths, the response is nearly constant with small incremental reductions in the bulging factor with the addition of stringers and frames. In this case, the crack is too small and too far to be affected by the stiffening elements. Figure 15 shows the effect of configuration for a longer crack, a = 8 in. In this case, the bulging factor is a nonlinear function of the applied pressure. In addition, the crack was long enough to be influenced by the stringers and frames. As shown in figure 15, there is a substantial reduction in the bulging factor for the longitudinally stiffened cases compared to the unstiffened lap joint case.

CONCLUDING REMARKS

In this study, the effects of bulging in aircraft structures containing a longitudinal lap splice joint were determined. A typical three-rivet row lap joint configuration containing a mid-bay crack in the critical rivet row was chosen and analyzed. The Modified Crack Closure Integral method was used to calculate crack tip stress-intensity factors (SIF). Parametric studies were done to examine the effects of crack length, applied pressure, and stiffening elements (stringers and frames) on the bulging factor. For short cracks, a near-constant response was obtained for the bulging factor as a function of the applied pressure. The presence of the stiffeners only slightly reduced the bulging factor for the shorter cracks. These cracks are too small and too far to be affected by the stiffening elements. For longer cracks, the bulging factor varied nonlinearly as a function of the applied pressure. The presence of the stiffeners significantly reduced the bulging factor, but not to the level that bulging can be neglected.

The bulging factor definition used in this study follows directly from the definition of bulging factor for unstiffened shells. While this definition is widely used for fuselage structures in published literature, it should be interpreted with care. The definition of bulging factor used, and shown in equation 7, is based solely upon K_1. The original definition was developed in the context of pressurized shells in which the loading is symmetric to the crack faces. This symmetry does not hold true for longitudinal lap splice joints. However, in all the configurations reported here, the results are K_1 dominant. Thus, the definition is a reasonably good estimator of the crack tip SIF and the bulging effect for the configurations presented in this report. Additionally, bulging factor, as noted previously, bundles the effect of curvature and the effect of stiffeners. In the definition of bulging factor, as shown in equation 7, the mode 1 SIF, K_1, is normalized with respect to $K_{1\ flat}$. Where $K_{1\ flat}$ is the mode 1 SIF at the tip of a crack in an infinite flat plate loaded with a far field tension equal to the hoop stress in the curved fuselage. This definition results in bulging factor (β) values less than 1. These values do not imply that the curvature of the fuselage reduces the SIF. These lower values are due to the stiffening effect of the longerons and stringers and are one consequence of bundling the geometry and stiffener effects in the definition of bulging factor.

Bulging factor is a decreasing function of the fuselage radius. In the fuselage geometries presented in this report the fuselage radius was kept constant among the lap joint configurations studied. Thus, the effect on bulging due to the variation in curvature of the fuselage structure is not demonstrated in this report. The effect of radius on bulging factor has not been studied for cracks in lap joints; it has, however, been studied in context of fuselages stiffened with straps. For details, see reference 6.

In this study, in addition to the bulging factor, the crack tip SIF for all the configurations considered were calculated and partitioned into the four Kirchoff SIFs. In a future study these values could be used as a starting point for an improved definition of bulging factor(s) for fuselage structures, which can have a wider applicability in damage tolerance and crack growth studies.

REFERENCES

1. Folias, E.S., "An Axial Crack in a Pressurized Cylindrical Shell," *International Journal of Fracture*, Vol. 1, 1965, pp. 104-113.

2. Erdogan, F. and Kibler, J.J., "Cylindrical and Spherical Shells With Cracks," *International Journal of Fracture Mechanics*, Vol. 5, 1969, pp. 229-237.

3. Riks, E., "Bulging Cracks in Pressurized Fuselages: A Numerical Study," National Aerospace Laboratories, Amsterdam, The Netherlands, NLR MP 87058 U, 1987.

4. Ansell, H., "Bulging of Cracked Pressurized Aircraft Structure," Technical Licentiate Dissertation, Department of Mechanical Engineering, Linkoping Institute of Technology, Linkoping, Sweden, 1988.

5. Chen, D. and Schijve, J., "Bulging of Fatigue Cracks in a Pressurized Aircraft Fuselages," Delft Institute of Technology, Delft, The Netherlands, LR-655, 1991.

6. Bakuckas, J.G., Jr., Nguyen, P.V., Bigelow, C.A., and Broek, D., "Bulging Factors for Predicting Residual Strength of Fuselage Panels," in *Proceedings of the Symposium - International Committee on Aeronautical Fatigue*, Vol. 1, Edinburgh, UK, EMAS, 1997.

7. "Recommendations for Regulatory Action to Prevent Widespread Fatigue Damage in the Commercial Aircraft," Airworthiness Assurance Working Group of Aviation Rulemaking Advisory Committee—Transport Aircraft and Engine Issues, Washington, DC, 1999.

8. Viz, M.J., Zehnder, A.T., and Bamford, J.D., "Fatigue Fracture of Thin Plates Under Tensile and Transverse Shear Stresses," in *Fracture Mechanics: ASTM STP 1256*, Vol. 26, W. G. Reuter, J. H. Underwood, and J. James C. Newman, eds., Philadelphia, PA, American Society for Testing and Materials, 1995.

9. Viz, M.J., Potyondi, D.O., and Zehnder, A.T., "Computation of Membrane and Bending Stress-Intensity Factors for Thin Cracked Plates," *International Journal of Fracture*, Vol. 72, 1995, pp. 21-38.

10. Rybicki, E.F. and Kanninen, M.F., "A Finite Element Calculation of Stress-Intensity Factors by a Modified Crack Closure Integral," *Engineering Fracture Mechanics*, Vol. 9, 1977, pp. 931-938.

11. Chen, D., "Bulging of Fatigue Cracks in a Pressurized Aircraft Fuselage," Ph.D Dissertation, Department of Aerospace Engineering, Delft University of Technology, Delft, The Netherlands, 1991.

12. ABAQUS, Version 5.8, Hibbitt, Karlsson, and Sorenson (HKS), Pawtucket, RI, 1998.

13. Swift, T., "Development of the Fail-Safe Design Features of the DC-10," in *Special Technical Publication 486*, Philadelphia, PA, American Society for Testing Materials, 1970, pp. 164-214.

14. "Metallic Materials Properties Development and Standardization (MMPDS)," DOT Report - DOT/FAA/AR-MMPDS-01, January 2003.

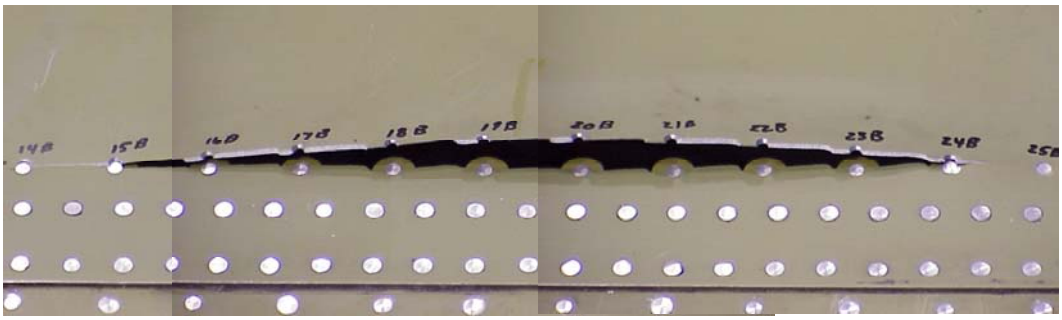

Crack in outer rivet row of a lap splice joint

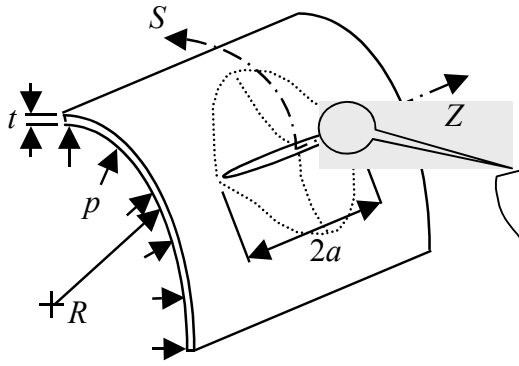

Bulging crack due to pressure

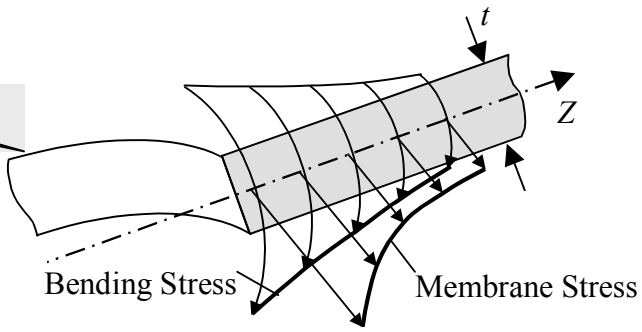

Stresses on crack plane

FIGURE 1. CRACK BULGING PHENOMENA

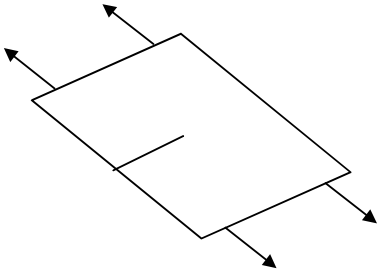

Symmetric Membrane Loading, K_1

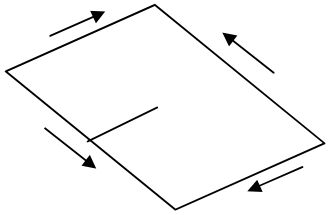

Antisymmetric Membrane Loading, K_2

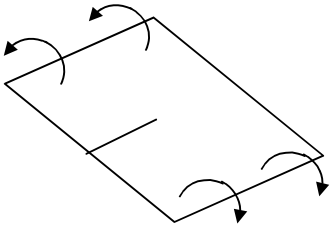

Symmetric Bending Loading, k_1

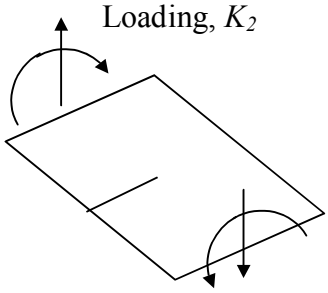

Antisymmetric Bending and Shear Loading, k_2

FIGURE 2. KIRCHOFF STRESS-INTENSITY FACTORS

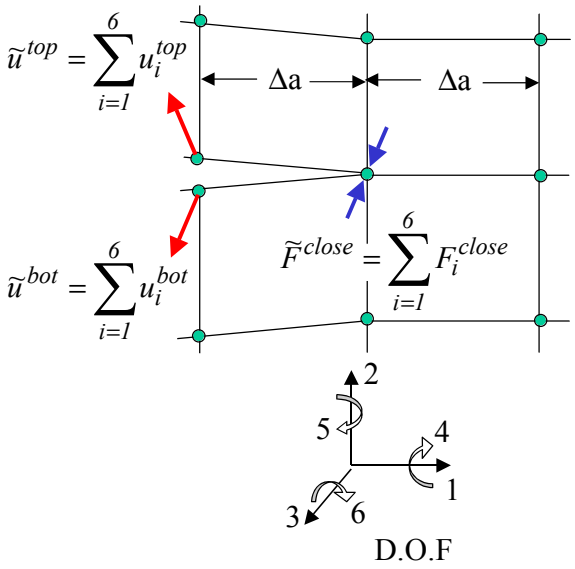

FIGURE 3. CRACK TIP FORCES AND DISPLACEMENTS NEEDED FOR MCCI METHOD

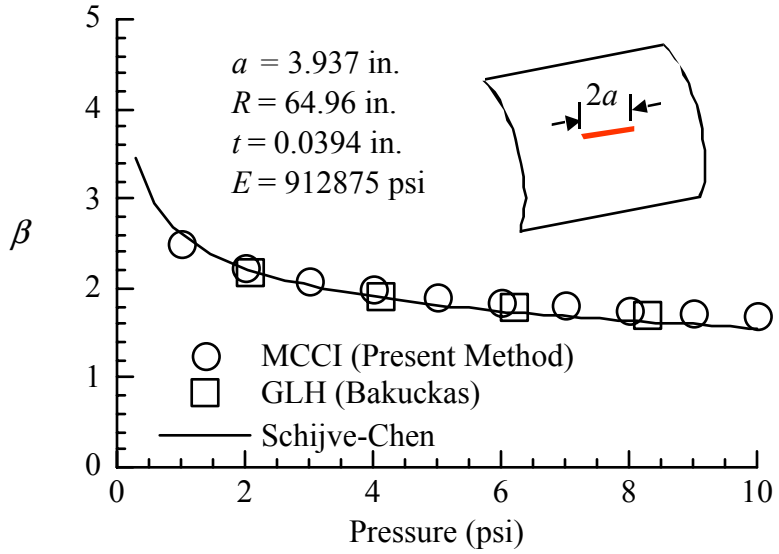

FIGURE 4. COMPARISON OF MCCI RESULTS WITH PUBLISHED SOLUTIONS

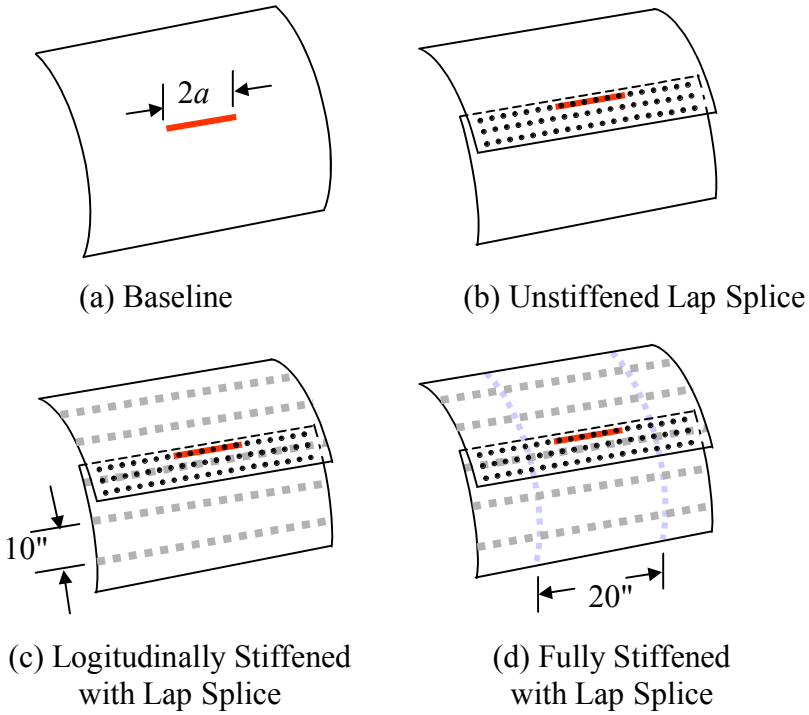

(a) Baseline

(b) Unstiffened Lap Splice

(c) Logitudinally Stiffened with Lap Splice

(d) Fully Stiffened with Lap Splice

FIGURE 5. FUSELAGE CONFIGURATIONS ANALYZED

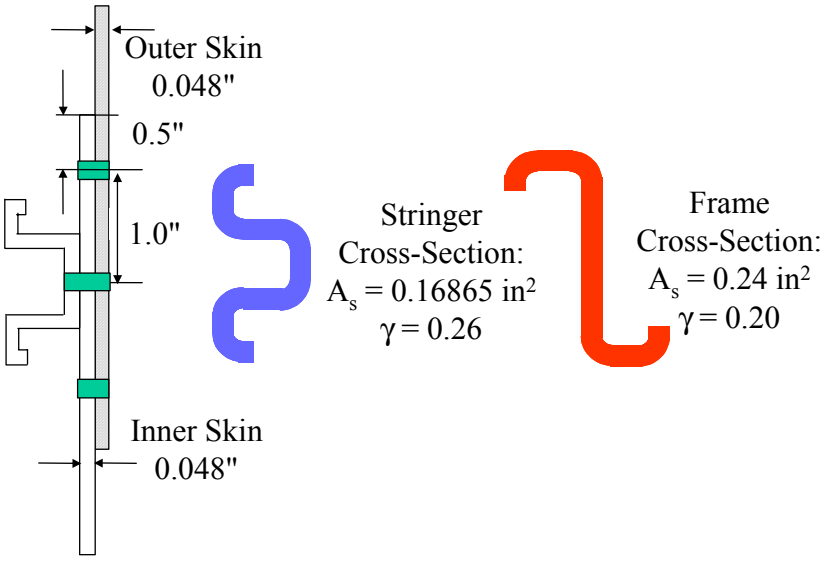

FIGURE 6. SUBSTRUCTURE DETAILS

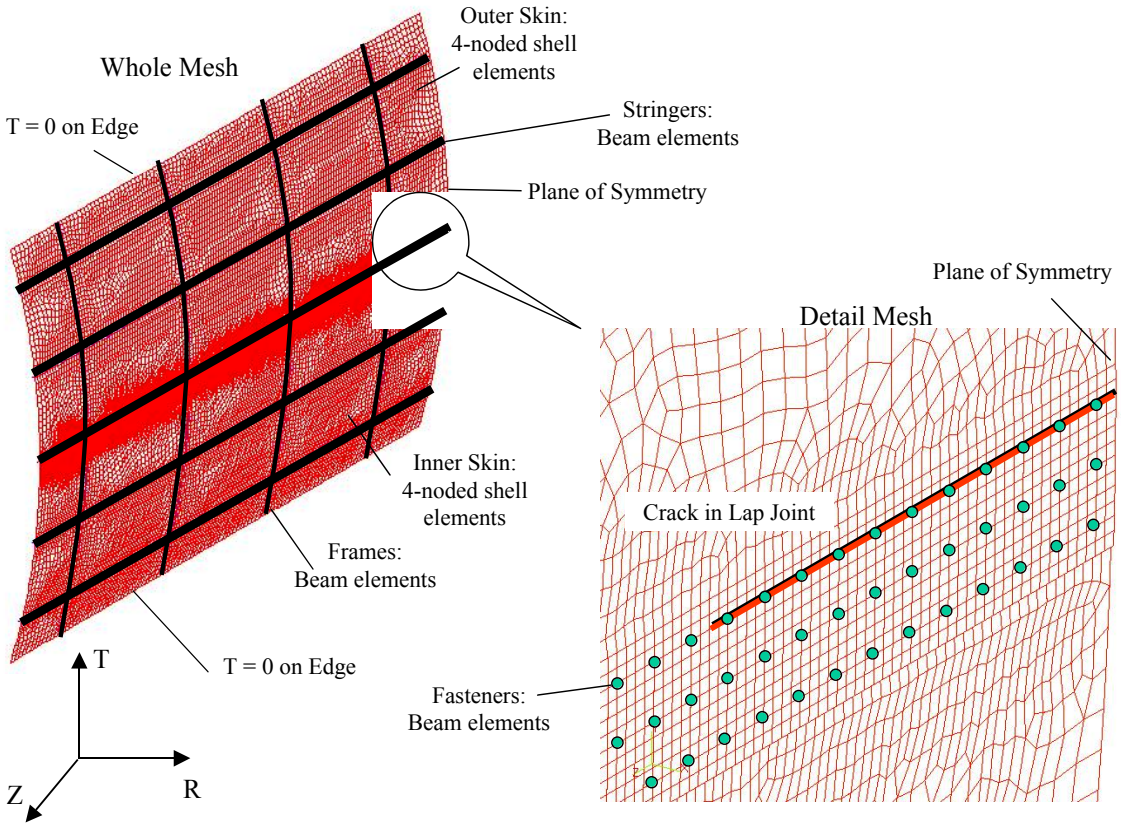

FIGURE 7. FINITE ELEMENT MESH

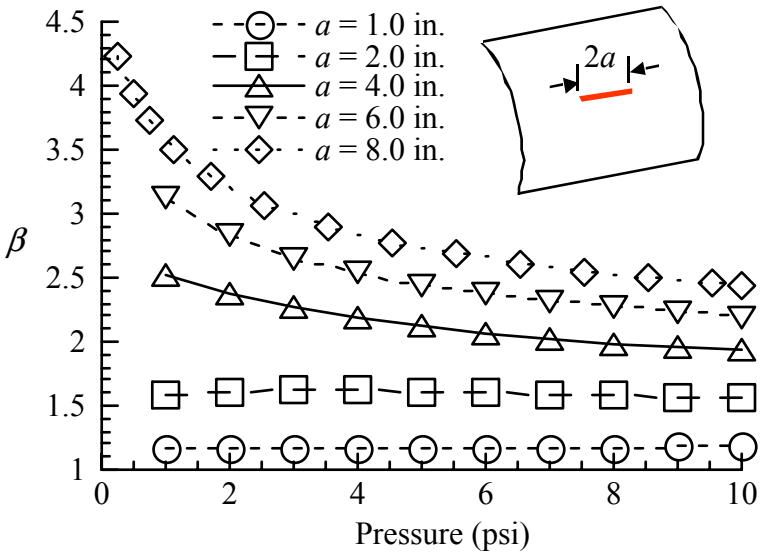

FIGURE 8. BULGING FACTOR AT THE TIP OF A LONGITUDINAL CRACK IN AN UNSTIFFENED FUSELAGE (R = 80 in.)

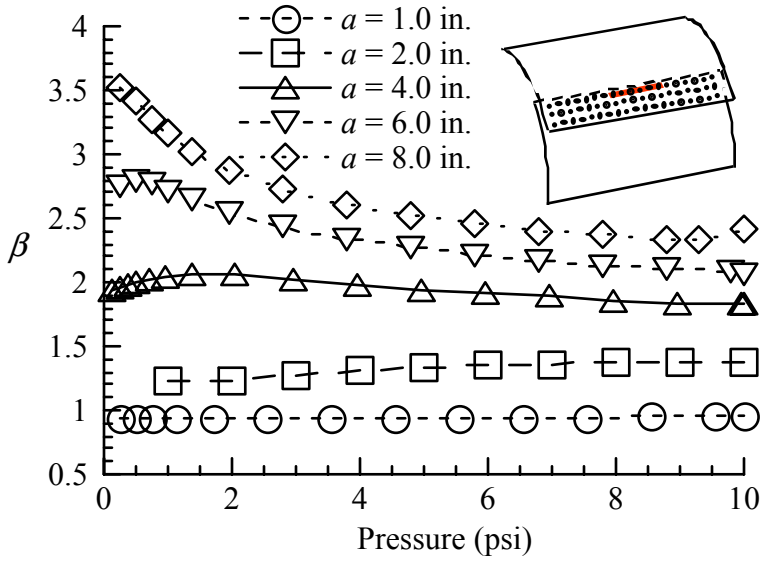

FIGURE 9. BULGING FACTORS AT THE TIP OF A LONGITUDINAL CRACK IN THE CRITICAL RIVET ROW OF A LAP SPLICE JOINT IN AN UNSTIFFENED FUSELAGE

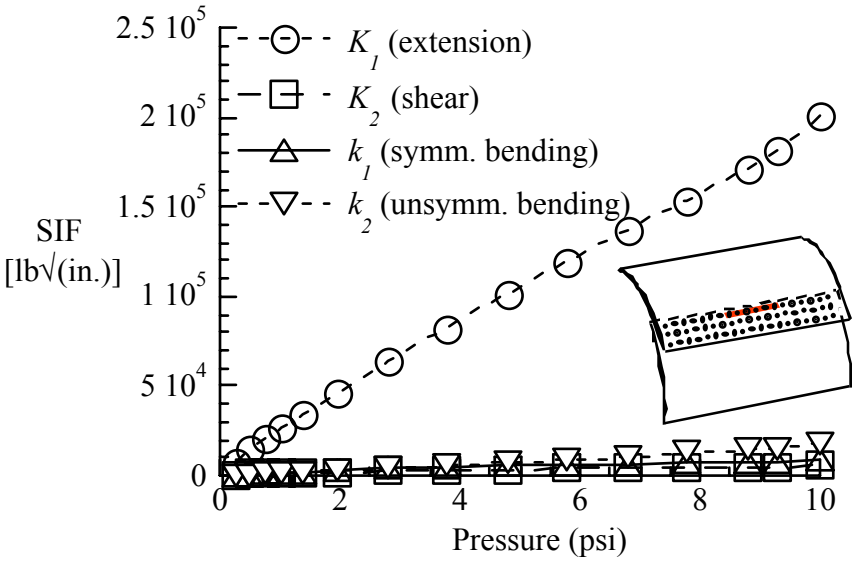

FIGURE 10. KIRCHOFF SIF AT THE TIP OF A CRACK, a = 8.0 in., IN THE CRITICAL RIVET ROW OF A LAP SPLICE JOINT IN AN UNSTIFFENED FUSELAGE (R = 80 in.)

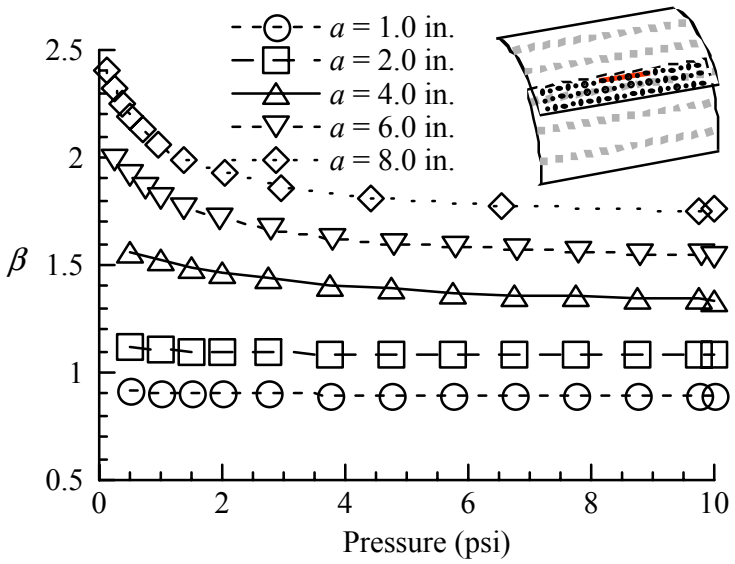

FIGURE 11. BULGING FACTORS AT THE TIP OF A CRACK IN THE CRITICAL RIVET ROW OF A LAP SPLICE JOINT IN A LONGITUDINALLY STIFFENED FUSELAGE (R = 80 in., Longeron Spacing = 10 in.)

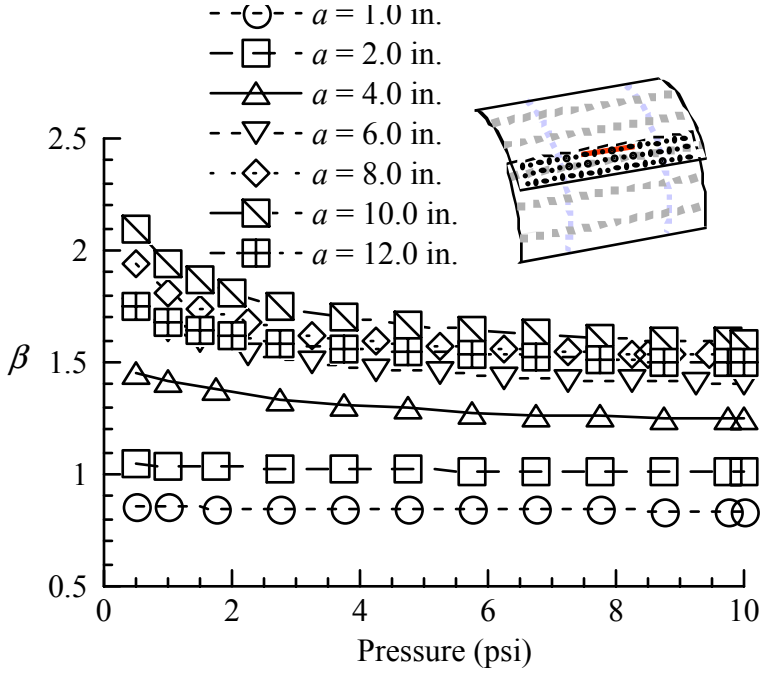

FIGURE 12. BULGING FACTORS AT THE TIP OF A CRACK IN THE CRITICAL RIVET ROW OF A LONGITUDINAL LAP SPLICE JOINT IN A FULLY STIFFENED FUSELAGE (R = 80 in., Longeron Spacing = 10 in., Frame Spacing = 20 in.)

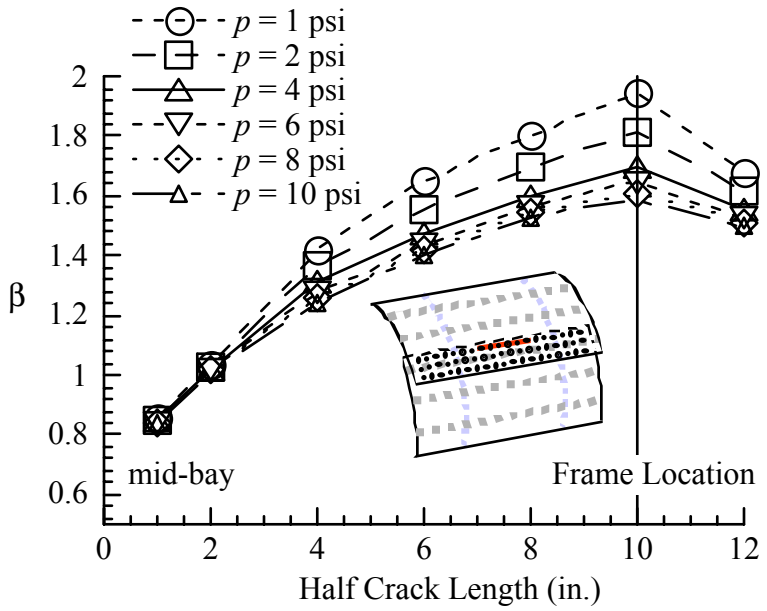

FIGURE 13. BULGING FACTOR AS A FUNCTION OF CRACK LENGTH FOR A FULLY STIFFENED FUSELAGE (R = 80 in., Longeron Spacing = 10 in., Frame Spacing = 20 in.)

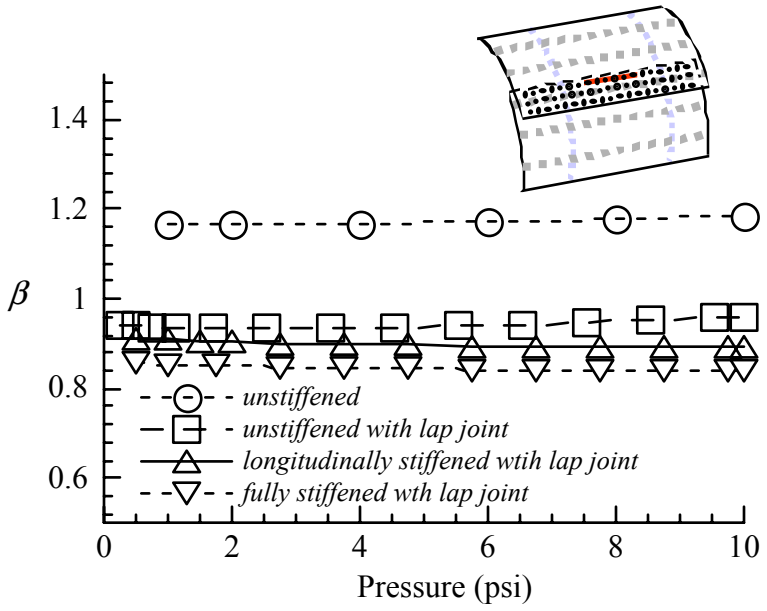

FIGURE 14. BULGING FACTOR FOR A LONGITUDINAL CRACK WITH a = 1 in. FOR THE CONFIGURATIONS ANALYZED

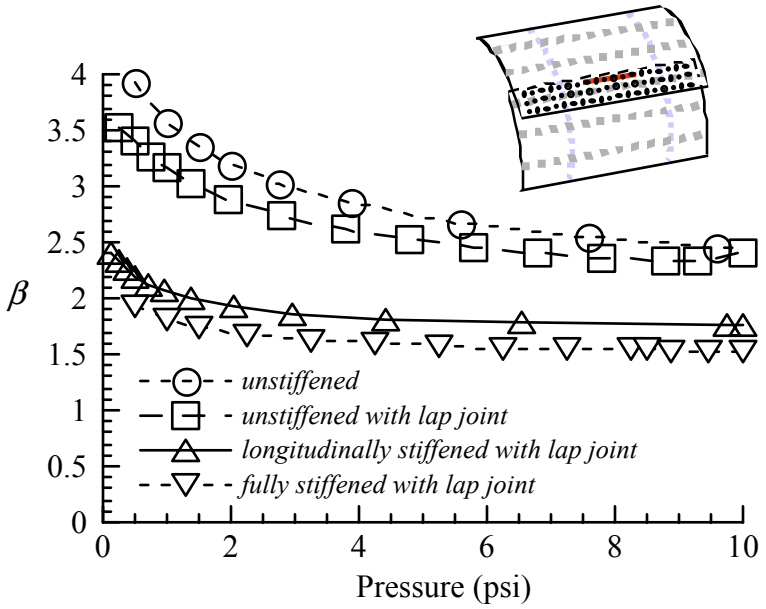

FIGURE 15. BULGING FACTOR FOR A LONGITUDINAL CRACK WITH a = 8 in. FOR THE CONFIGURATIONS ANALYZED

TABLE 1. MECHANICAL PROPERTIES REFERENCED FROM MMPDS-01

Component	Material	Thickness (in.)	Modulus of Elasticity (ksi)	Poisson's Ratio
Skin	2024-T3	0.048	10500	0.33
Stringer	7075-T6	0.048	10300	0.33
Frame	7075-T6	0.048	10300	0.33

TABLE 2. KIRCHOFF SIF AND β FOR A LONGITUDINAL CRACK IN AN UNSTIFFENED FUSELAGE WITH R = 80 in. AND a = 1.0 in.

p (psi)	$K_{1\,flat}$ $(\text{psi}\cdot\sqrt{\text{in}})$	K_1 $(\text{psi}\cdot\sqrt{\text{in}})$	K_2 $(\text{psi}\cdot\sqrt{\text{in}})$	k_1 $(\text{psi}\cdot\sqrt{\text{in}})$	k_2 $(\text{psi}\cdot\sqrt{\text{in}})$	β
1.00	2.954e+03	3.452e+03	0	4.820e+02	0	1.169
2.00	5.908e+03	6.897e+03	0	9.760e+02	0	1.168
3.00	8.862e+03	1.034e+04	0	1.492e+03	0	1.167
4.00	1.182e+04	1.381e+04	0	2.048e+03	0	1.168
5.00	1.477e+04	1.728e+04	0	2.630e+03	0	1.170
6.00	1.773e+04	2.078e+04	0	3.252e+03	0	1.172
7.00	2.068e+04	2.430e+04	0	3.903e+03	0	1.175
8.00	2.363e+04	2.785e+04	0	4.583e+03	0	1.178
9.00	2.659e+04	3.141e+04	0	5.284e+03	0	1.182
10.00	2.954e+04	3.501e+04	0	6.005e+03	0	1.185

TABLE 3. KIRCHOFF SIF AND β FOR A LONGITUDINAL CRACK IN AN UNSTIFFENED FUSELAGE WITH R = 80 in. AND a = 2.0 in.

p (psi)	$K_{1\,flat}$ $(\text{psi}\cdot\sqrt{\text{in}})$	K_1 $(\text{psi}\cdot\sqrt{\text{in}})$	K_2 $(\text{psi}\cdot\sqrt{\text{in}})$	k_1 $(\text{psi}\cdot\sqrt{\text{in}})$	k_2 $(\text{psi}\cdot\sqrt{\text{in}})$	β
1.00	4.178e+03	6.583e+03	0	1.874e+03	0	1.576
2.00	8.355e+03	1.342e+04	0	3.917e+03	0	1.607
3.00	1.253e+04	2.030e+04	0	5.721e+03	0	1.620
4.00	1.671e+04	2.704e+04	0	7.190e+03	0	1.618
5.00	2.089e+04	3.364e+04	0	8.395e+03	0	1.610
6.00	2.507e+04	4.010e+04	0	9.413e+03	0	1.600
7.00	2.924e+04	4.645e+04	0	1.029e+04	0	1.588
8.00	3.342e+04	5.271e+04	0	1.107e+04	0	1.577
9.00	3.760e+04	5.889e+04	0	1.178e+04	0	1.566
10.00	4.178e+04	6.500e+04	0	1.242e+04	0	1.556

TABLE 4. KIRCHOFF SIF AND β FOR A LONGITUDINAL CRACK IN AN UNSTIFFENED FUSELAGE WITH R = 80 in. AND a = 4.0 in.

p (psi)	$K_{1\,flat}$ $(\text{psi}\cdot\sqrt{\text{in}})$	K_1 $(\text{psi}\cdot\sqrt{\text{in}})$	K_2 $(\text{psi}\cdot\sqrt{\text{in}})$	k_1 $(\text{psi}\cdot\sqrt{\text{in}})$	k_2 $(\text{psi}\cdot\sqrt{\text{in}})$	β
1.00	5.908e+03	1.493e+04	0	5.244e+03	0	2.528
2.00	1.182e+04	2.805e+04	0	8.359e+03	0	2.374
3.00	1.773e+04	4.010e+04	0	1.036e+04	0	2.263
4.00	2.363e+04	5.155e+04	0	1.184e+04	0	2.181
5.00	2.954e+04	6.258e+04	0	1.304e+04	0	2.118
6.00	3.545e+04	7.330e+04	0	1.406e+04	0	2.068
7.00	4.136e+04	8.379e+04	0	1.495e+04	0	2.026
8.00	4.726e+04	9.408e+04	0	1.575e+04	0	1.990
9.00	5.317e+04	1.042e+05	0	1.647e+04	0	1.960
10.00	5.908e+04	1.142e+05	0	1.713e+04	0	1.933

TABLE 5. KIRCHOFF SIF AND β FOR A LONGITUDINAL CRACK IN AN UNSTIFFENED FUSELAGE WITH R = 80 in. AND a = 6.0 in.

p (psi)	$K_{1\,flat}$ $(\text{psi}\cdot\sqrt{\text{in}})$	K_1 $(\text{psi}\cdot\sqrt{\text{in}})$	K_2 $(\text{psi}\cdot\sqrt{\text{in}})$	k_1 $(\text{psi}\cdot\sqrt{\text{in}})$	k_2 $(\text{psi}\cdot\sqrt{\text{in}})$	β
1.00	7.236e+03	2.255e+04	0	8.374e+03	0	3.117
2.00	1.447e+04	4.089e+04	0	1.203e+04	0	2.825
3.00	2.171e+04	5.761e+04	0	1.421e+04	0	2.654
4.00	2.894e+04	7.340e+04	0	1.581e+04	0	2.536
5.00	3.618e+04	8.857e+04	0	1.709e+04	0	2.448
6.00	4.342e+04	1.033e+05	0	1.816e+04	0	2.379
7.00	5.065e+04	1.176e+05	0	1.910e+04	0	2.322
8.00	5.789e+04	1.316e+05	0	1.993e+04	0	2.274
9.00	6.512e+04	1.454e+05	0	2.067e+04	0	2.233
10.00	7.236e+04	1.590e+05	0	2.136e+04	0	2.198

TABLE 6. KIRCHOFF SIF AND β FOR A LONGITUDINAL CRACK IN AN UNSTIFFENED FUSELAGE WITH R = 80 in. AND a = 8.0 in.

p (psi)	$K_{1\,flat}$ ($\text{psi}\cdot\sqrt{\text{in}}$)	K_1 ($\text{psi}\cdot\sqrt{\text{in}}$)	K_2 ($\text{psi}\cdot\sqrt{\text{in}}$)	k_1 ($\text{psi}\cdot\sqrt{\text{in}}$)	k_2 ($\text{psi}\cdot\sqrt{\text{in}}$)	β
0.25	2.089e+03	8.816e+03	0	3.610e+03	0	4.220
0.50	4.178e+03	1.643e+04	0	7.319e+03	0	3.932
0.75	6.267e+03	2.334e+04	0	9.659e+03	0	3.725
1.12	9.400e+03	3.295e+04	0	1.199e+04	0	3.506
1.69	1.410e+04	4.630e+04	0	1.429e+04	0	3.284
2.53	2.115e+04	6.485e+04	0	1.657e+04	0	3.066
3.53	2.951e+04	8.543e+04	0	1.847e+04	0	2.895
4.53	3.786e+04	1.050e+05	0	1.993e+04	0	2.774
5.53	4.622e+04	1.239e+05	0	2.113e+04	0	2.682
6.53	5.457e+04	1.424e+05	0	2.216e+04	0	2.609
7.53	6.293e+04	1.605e+05	0	2.308e+04	0	2.550
8.53	7.128e+04	1.783e+05	0	2.390e+04	0	2.501
9.53	7.964e+04	1.958e+05	0	2.465e+04	0	2.459
10.00	8.355e+04	2.040e+05	0	2.499e+04	0	2.441

TABLE 7. KIRCHOFF SIF AND β IN THE CRITICAL RIVET ROW OF A LONGITUDINAL LAP SPLICE JOINT IN AN UNSTIFFENED FUSELAGE WITH R = 80 in. AND a = 1.0 in.

p (psi)	$K_{1\,flat}$ ($\text{psi}\cdot\sqrt{\text{in}}$)	K_1 ($\text{psi}\cdot\sqrt{\text{in}}$)	K_2 ($\text{psi}\cdot\sqrt{\text{in}}$)	k_1 ($\text{psi}\cdot\sqrt{\text{in}}$)	k_2 ($\text{psi}\cdot\sqrt{\text{in}}$)	β
0.25	7.380e+02	6.930e+02	1.600e+01	4.070e+02	5.200e+01	0.938
0.50	1.477e+03	1.386e+03	3.000e+01	6.470e+02	7.200e+01	0.938
0.75	2.216e+03	2.078e+03	4.200e+01	8.130e+02	5.900e+01	0.938
1.12	3.324e+03	3.113e+03	6.100e+01	9.870e+02	1.020e+02	0.937
1.69	4.987e+03	4.665e+03	8.700e+01	1.145e+03	2.390e+02	0.935
2.53	7.480e+03	6.992e+03	1.250e+02	1.247e+03	4.300e+02	0.935
3.53	1.043e+04	9.756e+03	1.690e+02	1.235e+03	6.540e+02	0.935
4.53	1.339e+04	1.253e+04	2.130e+02	1.096e+03	8.730e+02	0.936
5.53	1.634e+04	1.534e+04	2.560e+02	7.920e+02	1.080e+03	0.938
6.53	1.930e+04	1.817e+04	2.990e+02	4.100e+02	1.262e+03	0.942
7.53	2.225e+04	2.105e+04	3.410e+02	1.083e+03	1.410e+03	0.946
8.53	2.521e+04	2.398e+04	3.820e+02	1.537e+03	1.517e+03	0.951
9.53	2.816e+04	2.698e+04	4.200e+02	1.927e+03	1.580e+03	0.958
10.00	2.955e+04	2.840e+04	4.350e+02	2.172e+03	1.603e+03	0.961

TABLE 8. KIRCHOFF SIF AND β IN THE CRITICAL RIVET ROW OF A LONGITUDINAL LAP SPLICE JOINT IN AN UNSTIFFENED FUSELAGE WITH R = 80 in. AND a = 2.0 in.

p (psi)	$K_{1\,flat}$ ($\text{psi}\cdot\sqrt{\text{in}}$)	K_1 ($\text{psi}\cdot\sqrt{\text{in}}$)	K_2 ($\text{psi}\cdot\sqrt{\text{in}}$)	k_1 ($\text{psi}\cdot\sqrt{\text{in}}$)	k_2 ($\text{psi}\cdot\sqrt{\text{in}}$)	β
1.00	4.179e+03	5.116e+03	1.220e+02	8.610e+02	3.700e+02	1.224
2.00	8.358e+03	1.037e+04	2.550e+02	6.710e+02	9.720e+02	1.240
3.00	1.254e+04	1.593e+04	3.830e+02	5.630e+02	1.272e+03	1.271
4.00	1.672e+04	2.180e+04	4.540e+02	9.980e+02	1.259e+03	1.304
5.00	2.089e+04	2.781e+04	4.600e+02	1.218e+03	1.106e+03	1.331
6.00	2.507e+04	3.384e+04	4.110e+02	1.377e+03	9.050e+02	1.350
7.00	2.925e+04	3.985e+04	3.190e+02	1.525e+03	6.760e+02	1.362
8.00	3.343e+04	4.583e+04	2.360e+02	1.679e+03	6.780e+02	1.371
9.00	3.761e+04	5.177e+04	2.550e+02	1.843e+03	8.060e+02	1.376
10.00	4.179e+04	5.768e+04	2.620e+02	2.008e+03	9.520e+02	1.380

TABLE 9. KIRCHOFF SIF AND β IN THE CRITICAL RIVET ROW OF A LONGITUDINAL LAP SPLICE JOINT IN AN UNSTIFFENED FUSELAGE WITH R = 80 in. AND a = 4.0 in.

p (psi)	$K_{1\,flat}$ ($\text{psi}\cdot\sqrt{\text{in}}$)	K_1 ($\text{psi}\cdot\sqrt{\text{in}}$)	K_2 ($\text{psi}\cdot\sqrt{\text{in}}$)	k_1 ($\text{psi}\cdot\sqrt{\text{in}}$)	k_2 ($\text{psi}\cdot\sqrt{\text{in}}$)	β
0.13	7.380e+02	1.434e+03	6.300e+01	3.180e+02	1.100e+01	1.940
0.25	1.477e+03	2.890e+03	1.380e+02	4.570e+02	1.370e+02	1.956
0.37	2.216e+03	4.374e+03	2.230e+02	5.000e+02	2.990e+02	1.973
0.50	2.955e+03	5.886e+03	3.070e+02	4.790e+02	4.360e+02	1.992
0.69	4.063e+03	8.203e+03	4.090e+02	3.630e+02	5.700e+02	2.019
0.97	5.725e+03	1.174e+04	4.780e+02	2.060e+02	6.750e+02	2.051
1.39	8.219e+03	1.701e+04	4.540e+02	4.150e+02	8.100e+02	2.070
2.02	1.196e+04	2.462e+04	2.660e+02	1.820e+02	1.052e+03	2.059
2.97	1.757e+04	3.551e+04	4.160e+02	1.007e+03	1.408e+03	2.021
3.97	2.348e+04	4.648e+04	5.780e+02	1.562e+03	1.959e+03	1.980
4.97	2.939e+04	5.713e+04	6.970e+02	2.012e+03	2.625e+03	1.944
5.97	3.530e+04	6.754e+04	8.120e+02	2.401e+03	3.330e+03	1.913
6.97	4.121e+04	7.776e+04	9.190e+02	2.746e+03	4.002e+03	1.887
7.97	4.712e+04	8.782e+04	1.014e+03	3.058e+03	4.657e+03	1.864
8.97	5.303e+04	9.776e+04	1.091e+03	3.344e+03	5.270e+03	1.844
9.97	5.894e+04	1.076e+05	1.152e+03	3.612e+03	5.879e+03	1.825
10.00	5.910e+04	1.079e+05	1.132e+03	3.437e+03	5.869e+03	1.826

TABLE 10. KIRCHOFF SIF AND β IN THE CRITICAL RIVET ROW OF A LONGITUDINAL LAP SPLICE JOINT IN AN UNSTIFFENED FUSELAGE WITH R = 80 in. AND a = 6.0 in.

p (psi)	$K_{1\,flat}$ ($\mathrm{psi}\cdot\sqrt{\mathrm{in}}$)	K_1 ($\mathrm{psi}\cdot\sqrt{\mathrm{in}}$)	K_2 ($\mathrm{psi}\cdot\sqrt{\mathrm{in}}$)	k_1 ($\mathrm{psi}\cdot\sqrt{\mathrm{in}}$)	k_2 ($\mathrm{psi}\cdot\sqrt{\mathrm{in}}$)	β
0.25	1.810e+03	4.990e+03	4.180e+02	3.890e+02	1.860e+02	2.757
0.50	3.619e+03	1.013e+04	6.470e+02	1.120e+02	4.010e+02	2.798
0.75	5.429e+03	1.503e+04	7.250e+02	7.300e+01	6.040e+02	2.768
1.00	7.238e+03	1.967e+04	7.590e+02	5.430e+02	8.000e+02	2.717
1.37	9.953e+03	2.629e+04	7.810e+02	1.092e+03	1.191e+03	2.641
1.94	1.402e+04	3.567e+04	9.310e+02	1.755e+03	1.894e+03	2.544
2.78	2.013e+04	4.900e+04	1.233e+03	2.547e+03	3.049e+03	2.434
3.78	2.737e+04	6.408e+04	1.501e+03	3.289e+03	4.355e+03	2.341
4.78	3.461e+04	7.863e+04	1.675e+03	3.883e+03	5.557e+03	2.272
5.78	4.185e+04	9.280e+04	1.784e+03	4.381e+03	6.657e+03	2.218
6.78	4.908e+04	1.067e+05	1.841e+03	4.814e+03	7.683e+03	2.173
7.78	5.632e+04	1.203e+05	1.852e+03	5.204e+03	8.698e+03	2.136
8.78	6.356e+04	1.337e+05	1.807e+03	5.568e+03	9.756e+03	2.104
9.78	7.080e+04	1.470e+05	1.711e+03	5.910e+03	1.082e+04	2.076
10.00	7.238e+04	1.499e+05	1.632e+03	5.821e+03	1.101e+04	2.072

TABLE 11. KIRCHOFF SIF AND β IN THE CRITICAL RIVET ROW OF A LONGITUDINAL LAP SPLICE JOINT IN AN UNSTIFFENED FUSELAGE WITH R = 80 in. AND a = 8.0 in.

p (psi)	$K_{1\,flat}$ ($\mathrm{psi}\cdot\sqrt{\mathrm{in}}$)	K_1 ($\mathrm{psi}\cdot\sqrt{\mathrm{in}}$)	K_2 ($\mathrm{psi}\cdot\sqrt{\mathrm{in}}$)	k_1 ($\mathrm{psi}\cdot\sqrt{\mathrm{in}}$)	k_2 ($\mathrm{psi}\cdot\sqrt{\mathrm{in}}$)	β
0.25	2.089e+03	7.359e+03	6.810e+02	2.000e+02	1.610e+02	3.522
0.50	4.179e+03	1.425e+04	9.750e+02	3.790e+02	5.190e+02	3.409
0.75	6.268e+03	2.052e+04	1.155e+03	1.021e+03	8.620e+02	3.273
1.00	8.358e+03	2.642e+04	1.305e+03	1.554e+03	1.318e+03	3.161
1.37	1.149e+04	3.478e+04	1.662e+03	2.211e+03	2.115e+03	3.026
1.94	1.619e+04	4.664e+04	2.153e+03	2.998e+03	3.271e+03	2.880
2.78	2.325e+04	6.347e+04	2.761e+03	3.921e+03	4.850e+03	2.731
3.78	3.160e+04	8.248e+04	3.323e+03	4.765e+03	6.518e+03	2.610
4.78	3.996e+04	1.008e+05	3.762e+03	5.432e+03	7.999e+03	2.523
5.78	4.832e+04	1.187e+05	4.121e+03	6.003e+03	9.477e+03	2.457
6.78	5.668e+04	1.364e+05	4.407e+03	6.535e+03	1.116e+04	2.407
7.78	6.504e+04	1.540e+05	4.645e+03	7.034e+03	1.278e+04	2.368
8.78	7.339e+04	1.717e+05	4.875e+03	7.525e+03	1.438e+04	2.339
9.28	7.757e+04	1.809e+05	5.021e+03	7.727e+03	1.522e+04	2.332
10.00	8.358e+04	2.016e+05	6.318e+03	9.538e+03	1.844e+04	2.412

TABLE 12. KIRCHOFF SIF AND β IN THE CRITICAL RIVET ROW OF A LONGITUDINAL LAP SPLICE JOINT IN A LONGITUDINALLY STIFFENED FUSELAGE WITH R = 80 in. AND a = 1.0 in.

p (psi)	$K_{1\,flat}$ ($\text{psi}\cdot\sqrt{\text{in}}$)	K_1 ($\text{psi}\cdot\sqrt{\text{in}}$)	K_2 ($\text{psi}\cdot\sqrt{\text{in}}$)	k_1 ($\text{psi}\cdot\sqrt{\text{in}}$)	k_2 ($\text{psi}\cdot\sqrt{\text{in}}$)	β
0.50	1.477e+03	1.348e+03	2.700e+01	6.690e+02	3.900e+01	0.9122
1.00	2.955e+03	2.685e+03	4.700e+01	9.930e+02	1.530e+02	0.9085
1.50	4.432e+03	4.015e+03	6.500e+01	1.189e+03	2.980e+02	0.9058
2.00	5.910e+03	5.341e+03	8.000e+01	1.310e+03	4.490e+02	0.9038
2.75	8.126e+03	7.325e+03	1.010e+02	1.417e+03	6.710e+02	0.9015
3.75	1.108e+04	9.964e+03	1.250e+02	1.467e+03	9.730e+02	0.8992
4.75	1.404e+04	1.260e+04	1.460e+02	1.427e+03	1.293e+03	0.8974
5.75	1.699e+04	1.523e+04	1.640e+02	1.307e+03	1.623e+03	0.8961
6.75	1.995e+04	1.785e+04	1.790e+02	1.094e+03	1.961e+03	0.8951
7.75	2.290e+04	2.048e+04	1.920e+02	7.230e+02	2.307e+03	0.8943
8.75	2.586e+04	2.311e+04	2.030e+02	5.490e+02	2.660e+03	0.8936
9.75	2.881e+04	2.573e+04	2.130e+02	1.128e+03	3.019e+03	0.8932
10.00	2.955e+04	2.639e+04	2.130e+02	1.413e+03	3.150e+03	0.8931

TABLE 13. KIRCHOFF SIF AND β IN THE CRITICAL RIVET ROW OF A LONGITUDINAL LAP SPLICE JOINT IN A LONGITUDINALLY STIFFENED FUSELAGE WITH R = 80 in. AND a = 2.0 in.

p (psi)	$K_{1\,flat}$ ($\text{psi}\cdot\sqrt{\text{in}}$)	K_1 ($\text{psi}\cdot\sqrt{\text{in}}$)	K_2 ($\text{psi}\cdot\sqrt{\text{in}}$)	k_1 ($\text{psi}\cdot\sqrt{\text{in}}$)	k_2 ($\text{psi}\cdot\sqrt{\text{in}}$)	β
0.50	2.089e+03	2.331e+03	9.431e+01	8.308e+02	3.799e+02	1.115
1.00	4.179e+03	4.620e+03	1.831e+02	1.175e+03	1.023e+03	1.105
1.50	6.268e+03	6.890e+03	2.804e+02	1.340e+03	1.733e+03	1.099
2.00	8.358e+03	9.151e+03	3.912e+02	1.401e+03	2.477e+03	1.095
2.75	1.149e+04	1.253e+04	5.896e+02	1.378e+03	3.622e+03	1.091
3.75	1.567e+04	1.704e+04	9.139e+02	1.192e+03	5.151e+03	1.088
4.75	1.985e+04	2.155e+04	1.294e+03	8.030e+02	6.621e+03	1.086
5.75	2.403e+04	2.606e+04	1.710e+03	5.529e+02	7.985e+03	1.084
6.75	2.821e+04	3.056e+04	2.146e+03	1.167e+03	9.234e+03	1.083
7.75	3.239e+04	3.506e+04	2.589e+03	1.580e+03	1.037e+04	1.082
8.75	3.657e+04	3.955e+04	3.032e+03	1.923e+03	1.141e+04	1.082
9.75	4.074e+04	4.401e+04	3.496e+03	2.251e+03	1.223e+04	1.080
10.00	4.179e+04	4.513e+04	3.610e+03	2.451e+03	1.243e+04	1.080

TABLE 14. KIRCHOFF SIF AND β IN THE CRITICAL RIVET ROW OF A LONGITUDINAL LAP SPLICE JOINT IN A LONGITUDINALLY STIFFENED FUSELAGE WITH R = 80 in. AND a = 4.0 in.

p (psi)	$K_{1\,flat}$ ($\text{psi}\cdot\sqrt{\text{in}}$)	K_1 ($\text{psi}\cdot\sqrt{\text{in}}$)	K_2 ($\text{psi}\cdot\sqrt{\text{in}}$)	k_1 ($\text{psi}\cdot\sqrt{\text{in}}$)	k_2 ($\text{psi}\cdot\sqrt{\text{in}}$)	β
0.50	2.955e+03	4.595e+03	7.058e+02	9.169e+02	1.908e+03	1.555
1.00	5.910e+03	8.993e+03	1.573e+03	1.012e+03	3.779e+03	1.522
1.50	8.865e+03	1.322e+04	2.373e+03	8.811e+02	5.290e+03	1.491
2.00	1.182e+04	1.734e+04	3.093e+03	6.365e+02	6.575e+03	1.467
2.75	1.625e+04	2.336e+04	4.061e+03	3.324e+02	8.216e+03	1.438
3.75	2.216e+04	3.124e+04	5.203e+03	7.808e+02	1.006e+04	1.410
4.75	2.807e+04	3.900e+04	6.222e+03	9.769e+02	1.163e+04	1.389
5.75	3.398e+04	4.669e+04	7.154e+03	1.096e+03	1.300e+04	1.374
6.75	3.989e+04	5.434e+04	8.013e+03	1.189e+03	1.422e+04	1.362
7.75	4.580e+04	6.196e+04	8.794e+03	1.277e+03	1.544e+04	1.353
8.75	5.171e+04	6.960e+04	9.456e+03	1.379e+03	1.671e+04	1.346
9.75	5.762e+04	7.726e+04	1.004e+04	1.497e+03	1.796e+04	1.341
10.00	5.910e+04	7.920e+04	1.016e+04	1.694e+03	1.828e+04	1.340

TABLE 15. KIRCHOFF SIF AND β IN THE CRITICAL RIVET ROW OF A LONGITUDINAL LAP SPLICE JOINT IN A LONGITUDINALLY STIFFENED FUSELAGE WITH R = 80 in. AND a = 6.0 in.

p (psi)	$K_{1\,flat}$ ($\text{psi}\cdot\sqrt{\text{in}}$)	K_1 ($\text{psi}\cdot\sqrt{\text{in}}$)	K_2 ($\text{psi}\cdot\sqrt{\text{in}}$)	k_1 ($\text{psi}\cdot\sqrt{\text{in}}$)	k_2 ($\text{psi}\cdot\sqrt{\text{in}}$)	β
0.25	1.810e+03	3.588e+03	9.206e+02	6.855e+02	1.546e+03	1.983
0.50	3.619e+03	6.928e+03	1.884e+03	7.471e+02	2.965e+03	1.914
0.75	5.429e+03	1.009e+04	2.707e+03	6.355e+02	4.148e+03	1.858
1.00	7.238e+03	1.314e+04	3.425e+03	4.390e+02	5.179e+03	1.815
1.37	9.953e+03	1.758e+04	4.374e+03	2.762e+02	6.524e+03	1.766
1.94	1.402e+04	2.405e+04	5.606e+03	5.328e+02	8.237e+03	1.715
2.78	2.013e+04	3.350e+04	7.188e+03	4.029e+02	1.035e+04	1.664
3.78	2.737e+04	4.446e+04	8.804e+03	6.436e+02	1.239e+04	1.625
4.78	3.461e+04	5.537e+04	1.019e+04	1.064e+03	1.407e+04	1.600
5.78	4.185e+04	6.623e+04	1.142e+04	1.358e+03	1.559e+04	1.583
6.78	4.908e+04	7.701e+04	1.252e+04	1.548e+03	1.703e+04	1.569
7.78	5.632e+04	8.777e+04	1.346e+04	1.657e+03	1.839e+04	1.558
8.78	6.356e+04	9.852e+04	1.426e+04	1.696e+03	1.966e+04	1.550
9.78	7.080e+04	1.092e+05	1.497e+04	1.679e+03	2.081e+04	1.543
10.00	7.238e+04	1.116e+05	1.509e+04	1.410e+03	2.106e+04	1.542

TABLE 16. KIRCHOFF SIF AND β IN THE CRITICAL RIVET ROW OF A LONGITUDINAL LAP SPLICE JOINT IN A LONGITUDINALLY STIFFENED FUSELAGE WITH R = 80 in. AND a = 8.0 in.

p (psi)	$K_{1\,flat}$ ($\mathrm{psi}\cdot\sqrt{\mathrm{in}}$)	K_1 ($\mathrm{psi}\cdot\sqrt{\mathrm{in}}$)	K_2 ($\mathrm{psi}\cdot\sqrt{\mathrm{in}}$)	k_1 ($\mathrm{psi}\cdot\sqrt{\mathrm{in}}$)	k_2 ($\mathrm{psi}\cdot\sqrt{\mathrm{in}}$)	β
0.13	1.045e+03	2.515e+03	7.985e+02	5.182e+02	1.016e+03	2.407
0.25	2.089e+03	4.859e+03	1.629e+03	6.060e+02	2.013e+03	2.326
0.37	3.134e+03	7.064e+03	2.345e+03	5.472e+02	2.890e+03	2.254
0.50	4.179e+03	9.182e+03	2.969e+03	4.244e+02	3.675e+03	2.197
0.69	5.746e+03	1.225e+04	3.790e+03	1.084e+02	4.716e+03	2.132
0.97	8.097e+03	1.669e+04	4.850e+03	3.779e+02	6.060e+03	2.062
1.39	1.162e+04	2.314e+04	6.202e+03	3.451e+02	7.737e+03	1.991
2.02	1.691e+04	3.254e+04	7.918e+03	6.189e+02	9.753e+03	1.924
2.97	2.485e+04	4.628e+04	1.008e+04	1.333e+03	1.206e+04	1.863
4.40	3.675e+04	6.668e+04	1.268e+04	2.087e+03	1.455e+04	1.815
6.53	5.460e+04	9.702e+04	1.574e+04	2.813e+03	1.702e+04	1.777
9.74	8.137e+04	1.428e+05	1.853e+04	3.218e+03	1.953e+04	1.754
10.00	8.358e+04	1.468e+05	1.855e+04	2.668e+03	1.970e+04	1.757

TABLE 17. KIRCHOFF SIF AND β IN THE CRITICAL RIVET ROW OF A LONGITUDINAL LAP SPLICE JOINT IN A FULLY STIFFENED FUSELAGE WITH R = 80 in. AND a = 1.0 in.

p (psi)	$K_{1\,flat}$ ($\mathrm{psi}\cdot\sqrt{\mathrm{in}}$)	K_1 ($\mathrm{psi}\cdot\sqrt{\mathrm{in}}$)	K_2 ($\mathrm{psi}\cdot\sqrt{\mathrm{in}}$)	k_1 ($\mathrm{psi}\cdot\sqrt{\mathrm{in}}$)	k_2 ($\mathrm{psi}\cdot\sqrt{\mathrm{in}}$)	β
0.50	1.477e+03	1.264e+03	2.908e+01	6.171e+02	7.459e+01	0.8557
1.00	2.955e+03	2.524e+03	5.589e+01	9.821e+02	2.133e+02	0.8540
1.75	5.171e+03	4.401e+03	9.439e+01	1.301e+03	4.333e+02	0.8510
2.75	8.126e+03	6.889e+03	1.437e+02	1.514e+03	7.589e+02	0.8478
3.75	1.108e+04	9.367e+03	1.914e+02	1.591e+03	1.111e+03	0.8453
4.75	1.404e+04	1.184e+04	2.380e+02	1.583e+03	1.463e+03	0.8434
5.75	1.699e+04	1.431e+04	2.838e+02	1.511e+03	1.817e+03	0.8420
6.75	1.995e+04	1.677e+04	3.289e+02	1.380e+03	2.172e+03	0.8410
7.75	2.290e+04	1.924e+04	3.736e+02	1.179e+03	2.528e+03	0.8401
8.75	2.586e+04	2.171e+04	4.180e+02	8.715e+02	2.888e+03	0.8396
9.75	2.881e+04	2.418e+04	4.622e+02	1.420e+02	3.253e+03	0.8392
10.00	2.955e+04	2.479e+04	4.730e+02	6.973e+02	3.348e+03	0.8389

TABLE 18. KIRCHOFF SIF AND β IN THE CRITICAL RIVET ROW OF A LONGITUDINAL LAP SPLICE JOINT IN A FULLY STIFFENED FUSELAGE WITH R = 80 in. AND a = 2.0 in.

p (psi)	$K_{1\,flat}$ ($\mathrm{psi}\cdot\sqrt{\mathrm{in}}$)	K_1 ($\mathrm{psi}\cdot\sqrt{\mathrm{in}}$)	K_2 ($\mathrm{psi}\cdot\sqrt{\mathrm{in}}$)	k_1 ($\mathrm{psi}\cdot\sqrt{\mathrm{in}}$)	k_2 ($\mathrm{psi}\cdot\sqrt{\mathrm{in}}$)	β
0.50	2.089e+03	2.188e+03	8.095e+01	7.591e+02	5.455e+02	1.047
1.00	4.179e+03	4.341e+03	1.648e+02	1.153e+03	1.242e+03	1.039
1.75	7.313e+03	7.536e+03	3.165e+02	1.423e+03	2.382e+03	1.031
2.75	1.149e+04	1.177e+04	5.780e+02	1.483e+03	3.965e+03	1.024
3.75	1.567e+04	1.600e+04	9.060e+02	1.344e+03	5.538e+03	1.021
4.75	1.985e+04	2.022e+04	1.286e+03	1.047e+03	7.034e+03	1.019
5.75	2.403e+04	2.444e+04	1.700e+03	4.713e+02	8.418e+03	1.017
6.75	2.821e+04	2.866e+04	2.131e+03	8.576e+02	9.684e+03	1.016
7.75	3.239e+04	3.287e+04	2.569e+03	1.320e+03	1.084e+04	1.015
8.75	3.657e+04	3.708e+04	3.007e+03	1.669e+03	1.190e+04	1.014
9.75	4.074e+04	4.126e+04	3.462e+03	1.989e+03	1.274e+04	1.013
10.00	4.179e+04	4.230e+04	3.575e+03	2.170e+03	1.294e+04	1.012

TABLE 19. KIRCHOFF SIF AND β IN THE CRITICAL RIVET ROW OF A LONGITUDINAL LAP SPLICE JOINT IN A FULLY STIFFENED FUSELAGE WITH R = 80 in. AND a = 4.0 in.

p (psi)	$K_{1\,flat}$ ($\mathrm{psi}\cdot\sqrt{\mathrm{in}}$)	K_1 ($\mathrm{psi}\cdot\sqrt{\mathrm{in}}$)	K_2 ($\mathrm{psi}\cdot\sqrt{\mathrm{in}}$)	k_1 ($\mathrm{psi}\cdot\sqrt{\mathrm{in}}$)	k_2 ($\mathrm{psi}\cdot\sqrt{\mathrm{in}}$)	β
0.50	2.955e+03	4.298e+03	7.068e+02	8.258e+02	2.165e+03	1.454
1.00	5.910e+03	8.398e+03	1.569e+03	9.926e+02	4.080e+03	1.421
1.75	1.034e+04	1.426e+04	2.754e+03	8.488e+02	6.332e+03	1.379
2.75	1.625e+04	2.178e+04	4.106e+03	3.279e+02	8.697e+03	1.340
3.75	2.216e+04	2.912e+04	5.278e+03	6.071e+02	1.064e+04	1.314
4.75	2.807e+04	3.635e+04	6.330e+03	8.016e+02	1.229e+04	1.295
5.75	3.398e+04	4.349e+04	7.295e+03	8.717e+02	1.372e+04	1.280
6.75	3.989e+04	5.060e+04	8.187e+03	8.866e+02	1.498e+04	1.268
7.75	4.580e+04	5.765e+04	9.015e+03	8.766e+02	1.618e+04	1.259
8.75	5.171e+04	6.471e+04	9.744e+03	8.873e+02	1.743e+04	1.251
9.75	5.762e+04	7.179e+04	1.038e+04	9.206e+02	1.869e+04	1.246
10.00	5.910e+04	7.358e+04	1.052e+04	1.120e+03	1.902e+04	1.245

TABLE 20. KIRCHOFF SIF AND β IN THE CRITICAL RIVET ROW OF A LONGITUDINAL LAP SPLICE JOINT IN A FULLY STIFFENED FUSELAGE WITH R = 80 in. AND a = 6.0 in.

p (psi)	$K_{1\,flat}$ ($\text{psi}\cdot\sqrt{\text{in}}$)	K_1 ($\text{psi}\cdot\sqrt{\text{in}}$)	K_2 ($\text{psi}\cdot\sqrt{\text{in}}$)	k_1 ($\text{psi}\cdot\sqrt{\text{in}}$)	k_2 ($\text{psi}\cdot\sqrt{\text{in}}$)	β
0.50000	3619.0	6305.0	1853.0	668.30	3310.0	1.7420
1.00	7.238e+03	1.193e+04	3.398e+03	5.003e+02	5.673e+03	1.648
1.50	1.086e+04	1.729e+04	4.671e+03	2.135e+02	7.599e+03	1.593
2.25	1.629e+04	2.508e+04	6.302e+03	4.409e+02	9.973e+03	1.540
3.25	2.352e+04	3.520e+04	8.156e+03	4.647e+02	1.252e+04	1.496
4.25	3.076e+04	4.513e+04	9.771e+03	1.030e+03	1.459e+04	1.467
5.25	3.800e+04	5.505e+04	1.118e+04	1.434e+03	1.634e+04	1.449
6.25	4.524e+04	6.489e+04	1.245e+04	1.751e+03	1.793e+04	1.434
7.25	5.248e+04	7.468e+04	1.359e+04	1.987e+03	1.942e+04	1.423
8.25	5.972e+04	8.443e+04	1.459e+04	2.157e+03	2.083e+04	1.414
9.25	6.695e+04	9.417e+04	1.546e+04	2.275e+03	2.214e+04	1.406
10.00	7.238e+04	1.015e+05	1.605e+04	2.299e+03	2.305e+04	1.402

TABLE 21. KIRCHOFF SIF AND β IN THE CRITICAL RIVET ROW OF A LONGITUDINAL LAPSPLICE JOINT IN A FULLY STIFFENED FUSELAGE WITH R = 80 in. AND a = 8.0 in.

p (psi)	$K_{1\,flat}$ ($\text{psi}\cdot\sqrt{\text{in}}$)	K_1 ($\text{psi}\cdot\sqrt{\text{in}}$)	K_2 ($\text{psi}\cdot\sqrt{\text{in}}$)	k_1 ($\text{psi}\cdot\sqrt{\text{in}}$)	k_2 ($\text{psi}\cdot\sqrt{\text{in}}$)	β
0.50	4.179e+03	8.104e+03	2.872e+03	3.831e+02	4.308e+03	1.939
1.00	8.358e+03	1.511e+04	4.883e+03	3.224e+02	7.263e+03	1.808
1.50	1.254e+04	2.179e+04	6.517e+03	3.337e+02	9.640e+03	1.738
2.25	1.881e+04	3.148e+04	8.604e+03	7.291e+02	1.252e+04	1.674
3.25	2.716e+04	4.409e+04	1.097e+04	1.476e+03	1.552e+04	1.623
4.25	3.552e+04	5.662e+04	1.294e+04	2.012e+03	1.790e+04	1.594
5.25	4.388e+04	6.906e+04	1.468e+04	2.399e+03	1.980e+04	1.574
6.25	5.224e+04	8.147e+04	1.622e+04	2.668e+03	2.136e+04	1.560
7.25	6.060e+04	9.382e+04	1.759e+04	2.822e+03	2.273e+04	1.548
8.25	6.895e+04	1.062e+05	1.876e+04	2.869e+03	2.398e+04	1.540
8.50	7.104e+04	1.093e+05	1.899e+04	2.709e+03	2.427e+04	1.539
8.88	7.418e+04	1.140e+05	1.936e+04	2.645e+03	2.467e+04	1.537
9.44	7.888e+04	1.210e+05	1.989e+04	2.617e+03	2.522e+04	1.533
10.00	8.358e+04	1.279e+05	2.036e+04	2.551e+03	2.572e+04	1.531

TABLE 22. KIRCHOFF SIF AND β IN THE CRITICAL RIVET ROW OF A LONGITUDINAL LAP SPLICE JOINT IN A FULLY STIFFENED FUSELAGE WITH R = 80 in. AND a = 10.0 in.

p (psi)	$K_{1\,flat}$ ($\text{psi}\cdot\sqrt{\text{in}}$)	K_1 ($\text{psi}\cdot\sqrt{\text{in}}$)	K_2 ($\text{psi}\cdot\sqrt{\text{in}}$)	k_1 ($\text{psi}\cdot\sqrt{\text{in}}$)	k_2 ($\text{psi}\cdot\sqrt{\text{in}}$)	β
0.50	4.672e+03	9.772e+03	3.873e+03	3.992e+02	4.532e+03	2.091
1.00	9.344e+03	1.817e+04	6.332e+03	9.972e+02	7.544e+03	1.945
1.50	1.402e+04	2.612e+04	8.279e+03	1.530e+03	9.864e+03	1.864
2.00	1.869e+04	3.382e+04	9.954e+03	1.992e+03	1.174e+04	1.810
2.75	2.570e+04	4.506e+04	1.216e+04	2.618e+03	1.397e+04	1.753
3.75	3.504e+04	5.972e+04	1.470e+04	3.280e+03	1.615e+04	1.704
4.75	4.439e+04	7.419e+04	1.678e+04	3.705e+03	1.771e+04	1.672
5.75	5.373e+04	8.853e+04	1.841e+04	3.944e+03	1.892e+04	1.648
6.75	6.308e+04	1.027e+05	1.981e+04	4.050e+03	1.986e+04	1.629
7.75	7.242e+04	1.168e+05	2.102e+04	4.051e+03	2.063e+04	1.613
8.75	8.176e+04	1.309e+05	2.207e+04	3.950e+03	2.130e+04	1.601
9.75	9.111e+04	1.449e+05	2.289e+04	3.695e+03	2.205e+04	1.591
10.00	9.344e+04	1.485e+05	2.302e+04	2.985e+03	2.215e+04	1.589

TABLE 23. KIRCHOFF SIF AND β IN THE CRITICAL RIVET ROW OF A LONGITUDINAL LAP SPLICE JOINT IN A FULLY STIFFENED FUSELAGE WITH R = 80 in. AND a = 12.0 in.

p (psi)	$K_{1\,flat}$ ($\text{psi}\cdot\sqrt{\text{in}}$)	K_1 ($\text{psi}\cdot\sqrt{\text{in}}$)	K_2 ($\text{psi}\cdot\sqrt{\text{in}}$)	k_1 ($\text{psi}\cdot\sqrt{\text{in}}$)	k_2 ($\text{psi}\cdot\sqrt{\text{in}}$)	β
0.50	5.118e+03	8.941e+03	3.801e+03	1.083e+03	1.411e+03	1.747
1.00	1.024e+04	1.722e+04	6.250e+03	1.747e+03	3.395e+03	1.683
1.50	1.535e+04	2.523e+04	8.168e+03	2.232e+03	5.294e+03	1.643
2.00	2.047e+04	3.309e+04	9.787e+03	2.607e+03	7.126e+03	1.616
2.75	2.815e+04	4.468e+04	1.186e+04	3.053e+03	9.768e+03	1.587
3.75	3.839e+04	5.994e+04	1.410e+04	3.468e+03	1.315e+04	1.562
4.75	4.862e+04	7.507e+04	1.582e+04	3.674e+03	1.629e+04	1.544
5.75	5.886e+04	9.011e+04	1.716e+04	3.696e+03	1.912e+04	1.531
6.75	6.910e+04	1.051e+05	1.829e+04	3.536e+03	2.169e+04	1.521
7.75	7.933e+04	1.200e+05	1.926e+04	3.169e+03	2.405e+04	1.512
8.75	8.957e+04	1.349e+05	2.003e+04	2.502e+03	2.619e+04	1.506
9.75	9.980e+04	1.498e+05	2.061e+04	1.180e+03	2.815e+04	1.501
10.00	1.024e+05	1.536e+05	2.068e+04	1.715e+03	2.863e+04	1.501